

Sheet Metal Forming Simulation and Real World Tooling

Matt Clarke
Continental Tool and Die
Windsor, CA
mattc@fleetwoodmetal.com

Jeanne He
Forming Simulation Technology LLC
qingjeanne@gmail.com

Abstract

In a modern day draw simulation; our objective has always been to verify the formability of the deformed blank. We then utilize the output of the simulation to ascertain the forces required to form the part. Little time is spent attempting to verify if our design for the die is capable of reproducing these results. Most simulation assumes the tools are rigid. The real expertise comes when you can reproduce that scenario in an actual tool that makes parts in a consistent manner.

This study follows a real world die development and build project, where the initial tryout was completely different from the simulation results, binder deformation has played a key role which differs the simulation results in which all tools are assumed to be rigid. Further simulation with a flexible binder has been performed, also compared to the real world solutions that were developed to make a good part. This study also provides valuable information for exploring the next generation of forming simulation needs. A major advance in simulation technology would be to answer the question of how simulation can compensate for these inadequacies. Through this study, it is clear that optimization analysis for various tooling needs to be shortened the tooling process time and reduction of the cost is an obvious trend in the near future.

Introduction

Forming simulation has been playing an increasingly important role in the Tool and Die industry. It has evolved to a level where the accuracy of the simulation can be argued against the real life results. We would like to say that there is a 3% margin for human error making a simulation 97% accurate. In our study we have isolated some of the factors that make up this margin of error. Design Constraints: a die can be constrained by the size and stroke of the press tool it will run in.

1. Limitations of real world purchased components: Nitrogen springs force curve is not ideal for draw forming.

2. Strength of materials: forming pad (binder) deformation and deflection during deep drawing due to lack of support.
3. Variation in quality of forming steels: steel across multiple lots can vary in formability.

This study will analyze these factors and describe how a more advanced forming simulation can produce real world results that might nearly eliminate that 3% margin of error, which could cost thousands of dollars in design changes and in-press R&D.

Die Design and Setup

This case study starts with a very common component shown in Figure 1 of this final shape. The blank material is JSC270E. The blank thickness is 0.65mm. The dimensions of this part are 430mm (17") by 330 mm (13") with part depth of 160mm (6.25").

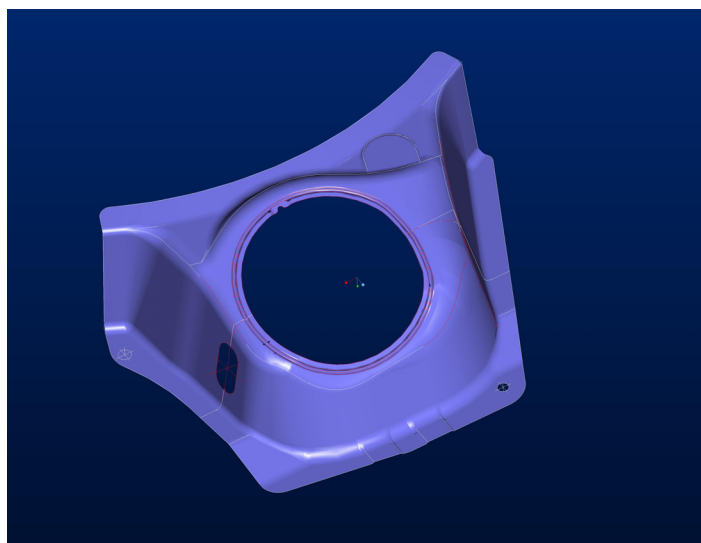


Figure 1: Product geometry

Process setup for this part is shown on the process sheet below:

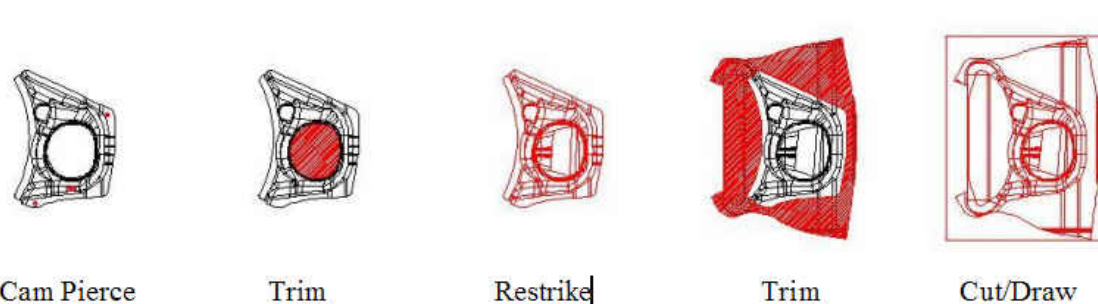


Figure 2: Process Layout

This part starts with a draw operation, which is a single action with a draw pad(binder), trim operation where the shaded portion are being trimmed, followed by a re-strike operation to firm the radius and small features. The fifth operation is the direct trim of the center area, followed by the final operation of the CAM piercing holes in the sidewall and flange area.

The major concern is the Draw Die design. Therefore simulation was conducted to support the draw die design. Figure 3. Shows the Draw Die set design

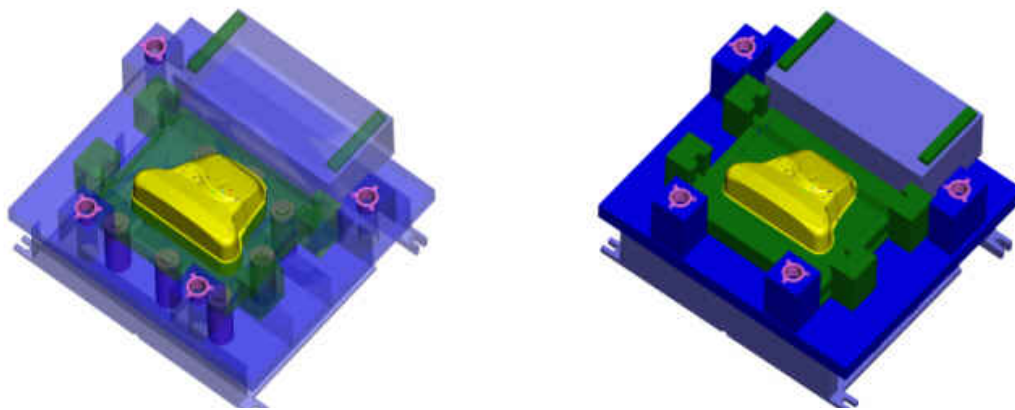


Figure 3: Draw Die design

Simulation with Rigid Tools

After sixteen (16) iterations of simulations and design changes, a clean simulation result have been obtained, Based on the simulation results, drawbead shape has been verified and tonnage was also determined. The draw pad (binder) tonnage prediction process includes the following:

1. Running simulation with displacement boundary condition for the binder travel.
2. Based on the calculated tonnage from this run.
3. Nitrogen cylinder type has been chosen and the cylinder numbers beneath the draw pad is being determined.
4. Running simulation that applies the tonnage curve matching the selected cylinder type, detailed tonnage curve is applied on the binder (Figure 5).

Cylinder position has been designed as shown in Figure 4. Nitrogen Cylinders are built into a nitrogen box, which is bolted to the underside of the die. The pins from the cylinders protrude through the shoe, and provide lift for the pad. There are 7 cylinders initially in this design. This will provide a force curve of 13.7 ton as initial value, and reaches 19.1 ton for final pressure.

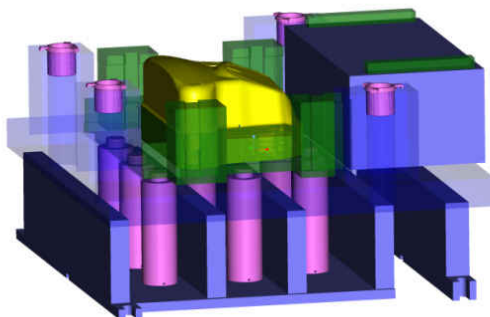


Figure 4: Nitrogen cylinders under the binder.

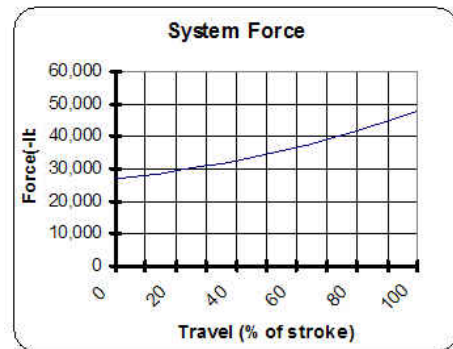


Figure 5: Cylinder tonnage information.

Tryout Reality

It took 12 weeks of draw die build and dry runs. The tool goes into the press, run tryout starts. When the draw was hit, the part exhibited a bad slip along the front of the part between the cutoff and the post areas. This unexpected flow was not indicated in the simulation (Figure 6). A clean draw was required before spotting could begin. Figure 7 shows a clean draw results with rigid tools, thickness plot shows good stretch in the front portion of the part, FLD plots shows compression inside the trimline in the front area.



Figure 7: Simulation results with rigid tools.

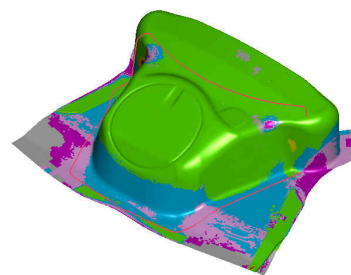


Figure 8: Simulation results with a solid binder for the original draw design

Tryout result shows problems in Figure 8, thickness plot shows low stretch in the front portion of the part and front portion drawbead mark is inside the trimline. FLD plot shows severe compression in the front area.

Identifying the Problem

Analysis the aforementioned problems, it is identified that the of the binder was flexing. In the area of the pad, where it had the least strength, the pad was actually bending open, casing

drawbead disengage, which allowed the material to flow. This was not predicted in the simulation. The shut height constraint that was put on the design did not allow for the pad to be made any thicker than it is. To solve this problem, an additional nitrogen cylinder was added to support the pad in the area where the flex occurred. This required some calculations to decrease the pressure in the entire nitrogen system (all the nitrogen cylinders are hosed together) so that the overall pressure curve would still be similar to that that was simulated. The result was a part that exhibited the same behavior as the rigid tool simulation.

The problem took three days of press time to diagnose, Two days of CNC setup and machining and three more days of press time, as well as some addition of components to fix. That adds up to thousands of dollars because of a margin of error that was not compensated for in the simulation.

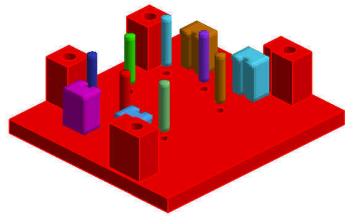


Figure 8: Cylinder pad and cylinders.

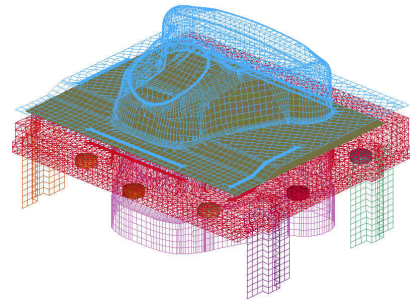


Figure 9: Simulation with a solid binder.

Simulation with a Deformable Binder

Can simulation help detect this problem at early stage of Die Design? How much more effort and CPU cost would be involved for this requirement. First of all, the binder has to be modeled as a deformable body. Due to the complexity of the binder geometry, especially the geometry bead on the top surface of the binder, Tetrahedron mesh is being used for the binder modeling. Punch and Die are both modeled as rigid body. Nitrogen cylinders (Figure 8) are modeled at the designed locations underneath the binder.

With LS-DYNA® explicit solver, material 18, the power law elasticity, is used for the solid binder, with element formulation 10, one point tetrahedron. Material 36, three-Parameter Barlet plasticity, is used for the Blank, with element formulation of 2, Belytschko-Tsay shell. Solid binder is modeled as supported by nitrogen cylinders on the bottom and four guide plates on both sides. All nitrogen cylinders are modeled with a rigid body stopper for the upper limit displacement constrains and provided force applied in the direction against the draw direction. Selective mass scaling is being used to reduce the high frequency numerical noise, thus reducing the kinetic energy caused by mass scaling.

First simulation with the solid binder is setup to predict original design. Simulation successfully predicts the problem shown on the tryout (Figure 7). Four sections as shown bellow are defined for binder deflection study (Figure 10 and Figure 11).

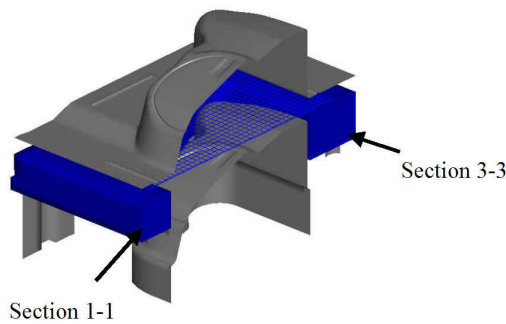


Figure 10: locations for section 1-1 and 3-3

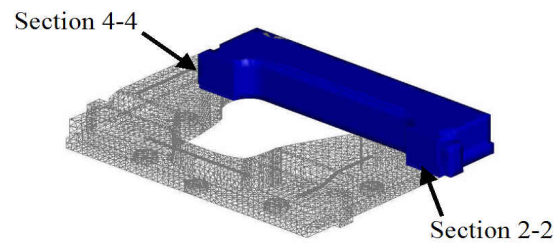


Figure 11: Locations for section 2-2 and 4-4

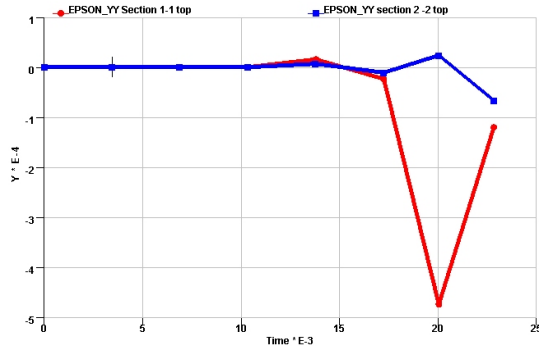


Figure 12: Longitudinal strain on section 1-1 and 3-3 top surfaces for the original design.

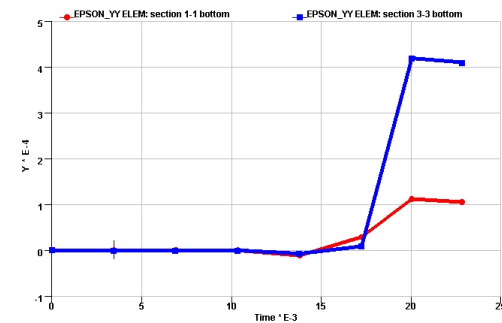


Figure 14: Longitudinal strain on section 1-1 and 3-3 bottom surfaces for the original design.

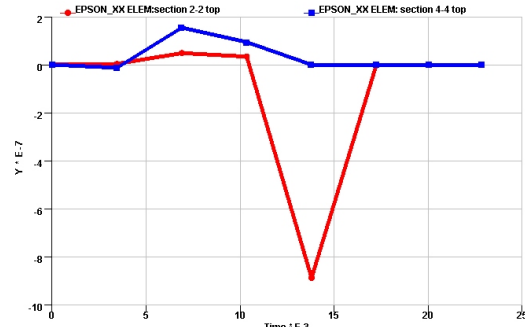


Figure 13: Longitudinal strain on section 2-2 and 4-4 top surfaces for the original design.

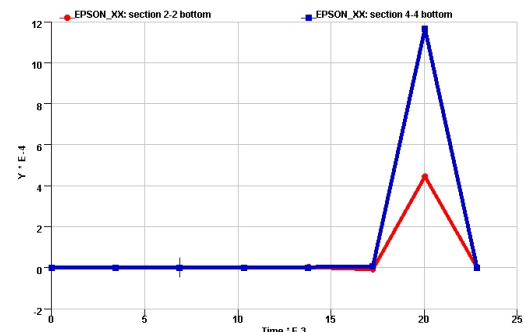


Figure 15: Longitudinal strain on section 2-2 and 4-4 bottom surfaces for the original design.

With the sections defined as shown above, LS-DYNA® analysis has been performed. As the deflection occurs happens at the time range of when upper die close with the binder, strain plots within that range have been studied in detail.

Figure 12 and Figure 14 show the longitudinal strain of the top and bottom surface for the section 1-1 and section 3-3 (Figure 10). Section 1-1 displays compression on the top surface and tension on the bottom surface. Section 2-2 has moderate compression on the top surface and

tension on the bottom surface. Quantitative evaluation shows the section 1-1 has high bending moments, which will induce the deflection of the binder, simulation shows 0.3 mm of deflection on section 1-1.

Figure 13 and Figure 15 shows the longitudinal strain of the top and bottom surface for the section 2-2 and section 4-4. Section 2-2 shows low compression on the top surface and tension on the bottom. Section 4-4 has low compression on the top surface; high tension on the bottom surfaces cased cylinder supports with no severe bending mode has been observed.

Simulation results clearly indicates section 1-1 is the area where deflection occurs, which agrees with the tryout findings, the next simulation is setup with an added nitro at the section 1-1 location, under the drawbead. With this new design, we can further simulate and analysis this case.

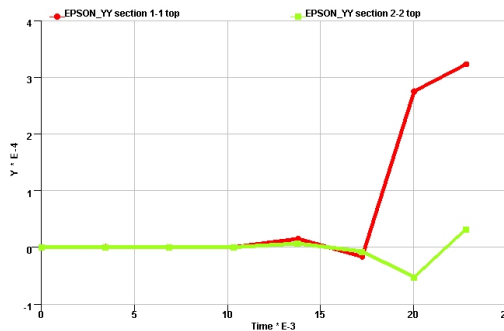


Figure 16: Longitudinal strain on section 1-1 and 3-3 top surfaces for the new design.

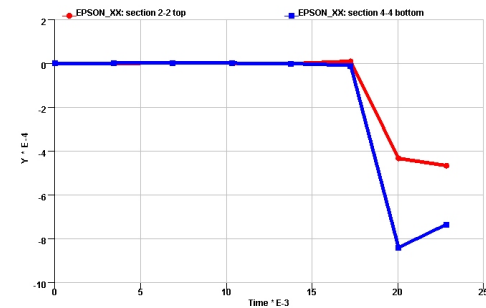


Figure 17: Longitudinal strain on section 2-2 and 4-4 top surfaces for the new design

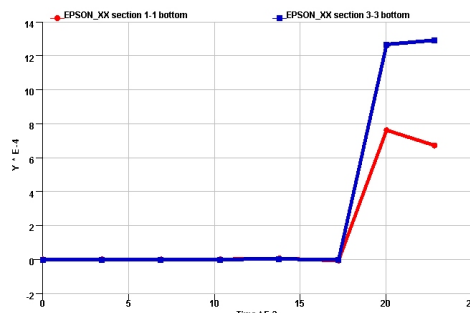


Figure 18: Longitudinal strain on section 1-1 and 3-3 bottom surfaces for the new

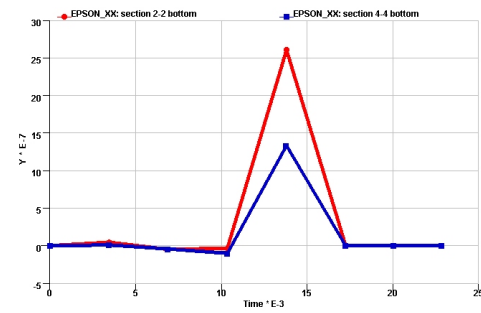


Figure 19: Longitudinal strain on section 2-2 and 4-4 bottom surfaces for the new design.

By comparing Figure 16 and Figure 12, it is clear that the compression on the top surface has been reduced with the additional nitro in the new design such that the severe bending mode has been eased to avoid the binder deflection. Figure 13 and 17 indicate that new design has higher compression on the section 4-4 top surfaces, with the high tension on the bottom surface of section 4-4(Figure 19). Deflection occurs on section 4-4, however, due to the drawbead is designed away from the section 4-4 location, and this deflection did not affect the material inflow in that local area.

Observations and Future Studies

Explicit analysis with solid binder in the draw simulation provides promising results for the prediction of binder deflections. It also provides realistic loading conditions for the binder deformation studies.

It is note that the CPU cost for the rigid tool is about 2 hours on a 2 GHz computer, while the cost of the solider binder is 8 hours.

Since all cylinders are hosed together, the tonnages provided from each cylinder are all equal (Figure 5). Figure 20 shows the contact force between the cylinders and the solid binder throughout the draw process. This plot indicates the unevenness of the impact between the binder and each cylinder. Can nitrogen cylinder locations and numbers of the nitrogen cylinder needed for the draw operation be optimized and determined? This will be further studied with LS-OPT®.

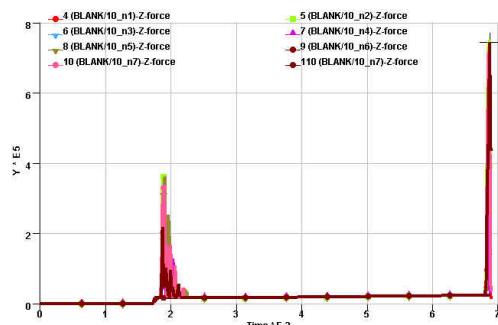


Figure 20: Contact force between the cylinders and binder.

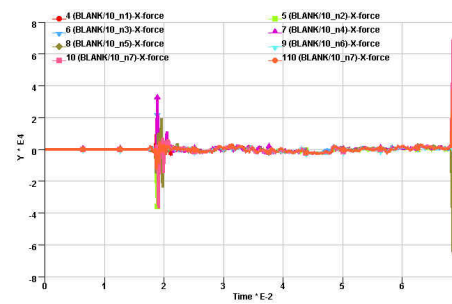


Figure 21: Side impact force on cylinders in x-direction.

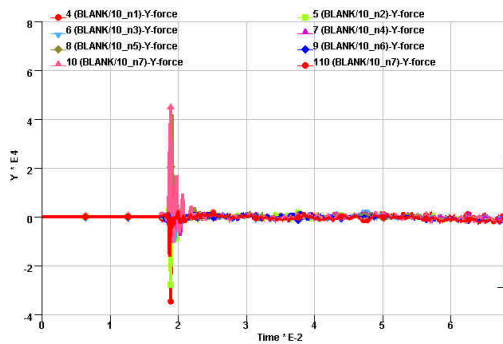


Figure 22: Side impact force on cylinders in y-direction

Figure 21 and Figure 22 shows the side force acted on each cylinder during the draw process. The graph shows significant side force impacted on cylinders in varies direction at different time of the draw stage. Adjusting cylinders to avoid sever side impact force preserve those costly stamping equipment is also a time consuming work in die shop. Can those be optimized with LS-DYNA and LS-OPT? Further-on study will be carried out to address this question.